2013 International Conference on Manipulation, Manufacturing and Measurement on the Nanoscale (3M-NANO)
26-30 August 2013, Suzhou, China

Mathematical Analysis for Controllable Near-Field Electrospinning

Jie Chen, Zhushuai Shao, Changhai Ru, Zhan Yang*
Jiangsu Key Laboratory for Advanced Robotics Technologies
Soochow University
Suzhou, China
*Correspondence author: yangzhan@suda.edu.cn

***Abstract*—Near-field electrospinning (NFES) is a novel method possessing higher controllability than conventional far-field electrospinning (FFES). But due to the lack of directions of theoretical model, precise deposition of nanofibers could only accomplished by experience. In this work, expressions for jet cross-sectional radius and jet velocity in NFES were derived in terms of axial position and initial jet acceleration. Based on nonlinear curve fitting method in MATLAB, an approximation for initial jet acceleration was acquired. With this model, it was able to accurately predict the diameter and velocity of nanofibers in NFES. Additionally, the movement speed of the workbench can be regulated by mathematical model rather than experience. So the model proposed in this paper had important guiding significance to precise deposition of nanofibers.**

Keywords—nonlinear curve fitting method; mathematical model; Near-field electrospinning

I. INTRODUCTION

Electrospinning is a straightforward, effective and convenient method to produce nanofibers from polymer solutions. These ultrathin fibers have revolved increasingly intense industrial and scientific interests due to their unique characteristics, such as small diameters and large surface area to volume ratio. Over the last few decades, electrospinning has been investigated for a wide range of applications, such as piezoelectric nanofibrous devices [1], drug delivery systems [2], solar energy applications [3], wound dressing [4], bio-scaffolds [5], sensors [6], membranes for filtration [7] and so on. Figure 1 explains the schematic of experimental setup for conventional electrospinning (FFES). As the electrical potential difference between the pendant polymer droplet and the grounded collector increases, the surface of the droplet becomes charged, with its shape altering from a circular one to a conical one referred to as the Taylor cone [8]. When the potential difference approaches its critical value that the electrical force imposed on the liquid droplet overcomes the surface tension force, a stable electrified jet emerges and electrospinning begins. Typically, in the electrospinning process, there are two stages. In the first stage, the electrified jet travels in a nearly straight line. And in the second stage, the jet begins to spiral and curl in space due to a "bending instability" [9]. Apparently, the controllability of far-field electrospinning (FFES) is limited because of its inherent instability. So it is very difficult to collect precisely deposited nanofibers in FFES.

Sun et al [10] reported a new type of electrospinning called near-field electrospinning (NFES) in 2006, figure 2 explains the schematic of experimental setup for near-field electrospinning (NFES). In order to utilize the stable stage of far-field electrospinning, they reduced the distance between the pipette and collector to the range of 500 to 3 mm. However, to deposit nanofibers precisely, the workbench should move at an appropriate speed determined by the final speed of the nanofiber. If the final speed of the nanofiber is faster than the collector moving speed, the fiber will spiral locally. When the collector moves faster than the nanofiber, the fiber may get diminished gradually. At present, due to the lack of directions of theoretical model, the movement speed of the workbench can only be adjusted by experience.

In this work, a mathematical model, having important guiding significance to precise deposition of nanofibers in NFES, has been proposed. With this model, it will be able to accurately predict the velocity of the electrified jet in NFES. Additionally, the movement speed of the workbench will be able to be regulated according to mathematical model rather than experience, so it will be more convenient and accurate.

In section 2, three unknown quantities of the charged jet in NFES, namely the cross-sectional radius, velocity and acceleration, are formulated in terms of axial position and initial jet acceleration. In section 3, based on nonlinear curve fitting method in MATLAB, an approximation for initial jet acceleration is acquired. Using this approximate value, the jet cross-sectional radius and jet velocity could be expressed in terms of axial coordinate. The results of the theoretical predictions are compared with experimental data, and agreement between experiment and theory is discussed. In section 4, the conclusions are given.

II. DERIVATION OF JET VELOCITY AND JET CROSS-SECTIONAL RADIUS

In NFES, the trajectory of the electrified jet is nearly straight, therefore, the liquid jet can be assumed to be extensional and axisymmetric along the external electric field line. After getting stable, the movement of the electrified jet in the electric field can be seen as one dimensional steady-state, then we can use one dimensional steady-state fluid model to analyze the behavior of the jet. Three equations, representing mass conservation, charge conservation and the linear momentum balance are provided in the below, respectively [11]:

$$\pi r^2 v = Q \tag{2.1}$$

This work was supported by National Natural Science Fund of China under Grant No. 61174087, Jiangsu Natural Science Funds for Distinguished Young Scholar under Grant No. BK2012005, and Qing Lan Project of Jiangsu Province.

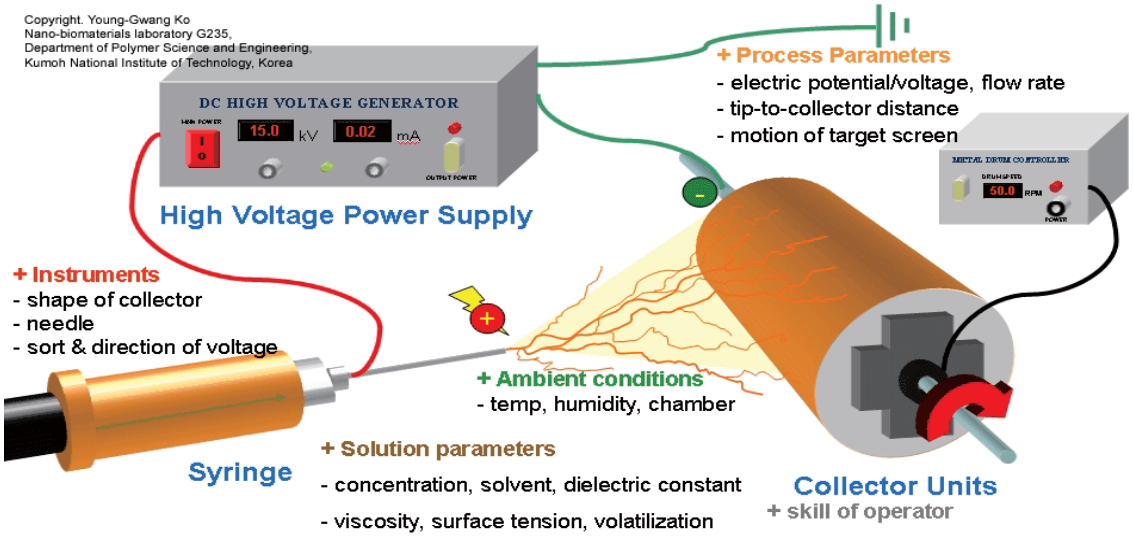

Fig. 1.Schematic of experimental setup for FFES (this picture comes from Google)

$$2\pi r\sigma v + k\pi r^2 E = I \tag{2.2}$$

$$\frac{d}{dz}\left(\frac{v^2}{2}\right) = -\frac{1}{\rho}\frac{dp}{dz} + g + \frac{2\sigma E}{\rho r} + \frac{d\tau}{dz} \tag{2.3}$$

Where Q is the volume flow rate of the solution, ρ is the density of the solution, r is the cross-sectional radius of the jet, v is the velocity of the jet, I is the total current in the electrified jet, E is the axial component of the electric field, k is the electric conductivity of the jet and σ is the surface charge density. As in NFES, the electrical forces imposed on the jet are dominant, then the other forces, such as the gravity, inertial, viscous, surface tension and hydrostatic forces can be ignored and equation (2.3) can be reduced to the following expression：

$$\frac{d}{dz}\left(\frac{v^2}{2}\right) = \frac{2\sigma E}{\rho r} \tag{2.4}$$

Assuming that the volumetric flow rate and the electric current of the jet are constant, (2.5), (2.6) and (2.7) can be derived:

$$v \propto r^{-2}, \sigma \propto r, E \propto r^{-2} \tag{2.5}$$

$$\frac{d}{dz}\left(r^{-4}\right) \propto r^{-2} \tag{2.6}$$

$$v \propto z \tag{2.7}$$

Because the axial acceleration, velocity as well as displacement of the charged jet are all functions of the time, then the following hypothesis can be made according to (2.7):

$$z = kv + b \tag{2.8}$$

Where k and b are coefficients determined by boundary conditions. According to derivation of both sides of (2.8) twice in a row, (2.9) is obtained:

$$a = \frac{dv}{dt} = \frac{d^2 z}{dt^2} = k\frac{d^2 v}{dt^2} = k\frac{da}{dt} \tag{2.9}$$

When *t*=0, $a(0) = a_0, v(0) = v_0 = Q/(\pi r_0^2)$, $z(0) = 0$, therefore, by combination of (2.8) and (2.9), equation (2.10) and (2.11) can be derived:

$$v = \frac{\pi r_0^2 \cdot a_0 \cdot z}{Q} + \frac{Q}{\pi r_0^2} = \frac{a_0}{v_0} \cdot z + v_0 \tag{2.10}$$

$$r = r_0 \times \left(\frac{\pi^2 r_0^4 a_0}{Q^2} z + 1\right)^{-\frac{1}{2}} = r_0 \times \left(\frac{a_0}{v_0^2} \cdot z + 1\right)^{-\frac{1}{2}} \tag{2.11}$$

To make (2.10) and (2.11) dimensionless, dimensionless velocity $\tilde{v} = v/v_0$, radius $\tilde{r} = r/r_0$ and axial position $\tilde{z} = z/r_0$ are introduced and (2.12) and (2.13) can be acquired:

$$\tilde{z} = \beta \cdot \tilde{z} + 1 \tag{2.12}$$

$$\tilde{r} = \left(\beta \cdot \tilde{z} + 1\right)^{-1/2} \tag{2.13}$$

Where $\beta = a_0 \cdot r_0 / v_0^2$, r_0 is the internal radius of the metallic pipette, $v_0 = Q/\pi r_0^2$ is the initial velocity of the charged jet, a_0 is the initial jet acceleration. Once the value of β is calculated, functions for jet cross-sectional radius and jet velocity in NFES can be obtained. With these functions, the diameters and velocities of the nanofibers in NFES can be predicted accurately. Additionally, the movement speed of the workbench can be regulated according to results of mathematical calculation rather than experience. Therefore, it will be more accurate and convenient to deposit nanofibers in

NFES precisely.

In next section, PEO and PLGA are used as materials to conduct several experiments. In each experiment, nonlinear curve fitting method in MATLAB is applied to analyze the measured data and values of β are provided for each independent experiment, respectively. And agreement between theoretical model and experimental results is discussed.

III. EXPERIMENTAL SECTION

A. Materials and Process Parameters

Polyethylene oxide (PEO, molecular weight M=10^6g/mol) and Poly (lactic-co-glycolic acid) (PLGA, LA/GA 50/50, Mw = 40,000) were used to prepared polymer solutions. PEO was dissolved in a mixture of 60% deionized water and 40% ethano, PLGA was dissolved in a mixture of THF and NN-Dimethyl-formamide with a volume ratio of 3:1. All the solutions were stirred at room temperature using a magnetic stirrer for 18–24 h to ensure complete dissolution and obtain homogeneous solutions. The prepared solutions were kept in sealed containers at room temperature.

B. Experimental Setup

In NFES, several devices were required, including a metallic pipette with an internal diameter of about 160μm, a syringe pump (KD Scientific Inc, Holliston, American) to provide polymer solution for the experiment, a high voltage direct current power supply (Tianjin Dongwen High-Voltage Power Supply Co., Ltd, Tianjin China) with its negative electrode connected to the grounded collector and positive electrode connected to the pipette, a silicon collector, an X-Y motion stage, a light source, a microscope(Nikon ECLIPSE TS 100-F,Nikon,Tokyo, Japan) and a CCD camera (RENUSCO DTM-300,Suzhou,China)

C. Calculation of β Based on Nonlinear Curve Fitting Method in MATLAB

- Experiments conducted with PEO

The concentrations of the PEO solutions were 4wt% and 8wt%, respectively, and the volume flow rate was 0.5ml/h. Using nonlinear least squares method in MATLAB, an pproximation for was acquired. Theoretical curves and experimental data were shown in figure 3.

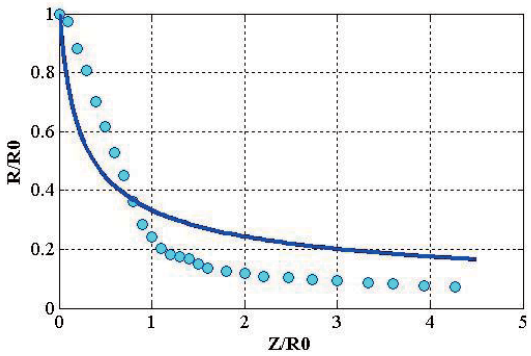

(a)

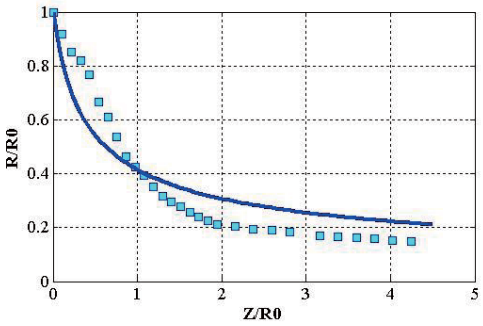

(b)

Fig.3.(a) 4wt% PEO solution. (b) 8wt% PEO solution. The dots referred to experimental results and the solid lines referred to fitting curves

The approximate value for was 7.96 with regard to 4wt% PEO solution and 2.89 for 8wt% PEO solution. Inserting the value of into equation (2.12) and (2.13), the following expressions for jet cross-sectional radius and jet velocity could be acquired:

4wt% PEO solution:

$$\tilde{r}_{4wt\%} = (7.96 \cdot \tilde{z} + 1)^{-1/2}$$

$$\tilde{v}_{4wt\%} = 7.96 \cdot \tilde{z} + 1$$

8wt% PEO solution:

$$\tilde{r}_{4wt\%} = (2.89 \cdot \tilde{z} + 1)^{-1/2}$$

$$\tilde{v}_{4wt\%} = 2.89 \cdot \tilde{z} + 1$$

It could be seen from figure 3 that at the origin of the jet, the theoretical curves failed to accurately tally with the experimental data. But as z / r_0 increased, the error between them decreased gradually.

- Experiments conducted with PLGA

The volume flow rates of PLGA solution were 0.5ml/h and 0.7ml/h, respectively. The mass to volume ratio was 0.3g/ml. Using nonlinear least squares method in MATLAB, an approximation for was acquired. The theoretical curves and experimental data were shown in figure 4.

volumetric flow rate 0.5ml/h:

$$\tilde{r}_{0.5ml/h} = (10.23 \cdot \tilde{z} + 1)^{-1/2},$$

$$\tilde{v}_{0.5ml/h} = 10.23 \cdot \tilde{z} + 1.$$

volumetric flow rate 0.7ml/h:

$$\tilde{r}_{0.7ml/h} = (5.06 \cdot \tilde{z} + 1)^{-1/2},$$

$$\tilde{v}_{0.7ml/h} = 5.06 \cdot \tilde{z} + 1.$$

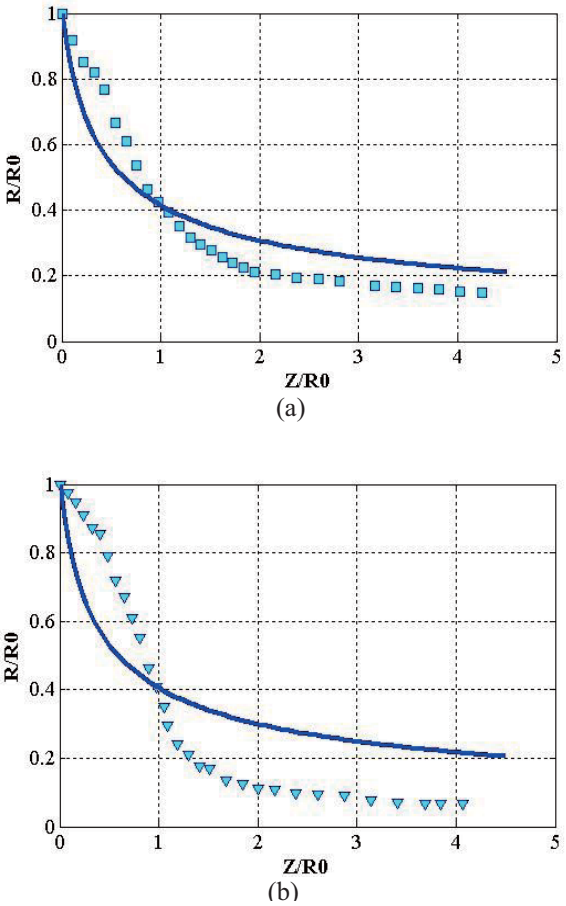

Fig.4.(a) PLGA solution with 0.5ml/h volume flow rate. (b) PLGA solution with 0.7ml/h volume flow rate. The dots referred to experimental results and the solid lines referred to fitting curves.

It could be obviously seen from figure 4 that as z / r_0 increased, the agreement between the theoretical curves and the experimental data increased at the same time. In this section, several separate experiments were carried out, which were PEO solution with different concentrations and PLGA solutions with different flow rates. Position parameters were acquired by contrasting experimental data with using nonlinear least squares method. It was found that theoretical curve can match the experimental data well. So using this model, we could predict the final dimension radius and the final speed of the NFES nanofibers accurately. Therefore, the model has guiding significance for controllable NFES.

IV. CONCLUSIONS

Near-field electrospinning (NFES) possesses higher controllability than far-field electrospinning (FFES). But due to the lack of directions of theoretical model, precise deposition of nanofibers could only accomplished by experience. In this work, expressions for jet cross-sectional radius and jet velocity were derived in terms of axial coordinate and initial jet acceleration. In order to calculate the initial jet acceleration, nonlinear curve fitting based on least squares method in MATLAB was used and an approximation for initial jet acceleration was acquired. With this model, it was able to accurately predict the diameter and velocity of the nanofibers in NFES. Additionally, the movement speed of the workbench can be regulated by mathematical model rather than experience. So the model proposed in this paper had important guiding significance to precise deposition of nanofibers.

ACKNOWLEDGMENT

The authors gratefully acknowledge financial support from National Natural Science Fund of China under Grant No. 61174087, Jiangsu Natural Science Funds for Distinguished Young Scholar under Grant No. BK2012005, and Qing Lan Project of Jiangsu Province.

REFERENCES

[1] C. Chang, V.H. Tran, J. Wang, Y.K.Fuh and L. Lin, “Direct-write piezoelectric polymeric nanogenerator with high energy conversion efficiency,”Nano letters, vol.10,pp.726-731,2010.

[2] W. Cui, Y. Zhou and J. Chang,“Electrospunnanofibrous materials for tissue engineering and drug delivery,”Science and Technology of Advanced Materials, vol.11,2010.

[3] M.Grätzel, “Dye-sensitized solid-state heterojunction solar cells,”MRS Bull, vol.30, pp. 23-27, 2005.

[4] H.J. Jin, S.V.Fridrikh, G.C. Rutledge and D.L.Kaplan, “ElectrospinningBombyxmori silk with poly (ethylene oxide),” Biomacromolecules, vol.3, pp.1233-1239,2002.

[5] S.Y. Chew, R.Mi, A.Hoke and K.W.Leong, “The effect of the alignment of electrospun fibrous scaffolds on Schwann cell maturation,” Biomaterials, vol.29, pp. 653-661,2008.

[6] J.S Im, S.C Kang, S.H Lee and Y.S Lee,“Improved gas sensing of electrospun carbon fibers based on pore structure, conductivity and surface modification,”Carbon, vol.48, pp.2573-2581, 2010.

[7] Y.C.Ahn, S.K. Park, G.T. Kim, Y.J. Hwang,C.G. Lee, H.S. Shin and J.K.Lee, “Development of high efficiency nanofilters made of nanofibers,”Current Applied Physics, vol.6, pp.1030-1035, 2006.

[8] G.Taylor, “Electrically driven jets Proceedings of the Royal Society of London,” A. Mathematical and Physical Sciences,vol.313, pp.453-475,1969.

[9] J. J.Feng, “The stretching of an electrified non-Newtonian jet: A model for electrospinning,”Physics of Fluids,vol.14,pp.3912-3926,2002.

[10] D. Sun,C. Chang, S. Li and L. Lin,“Near-field electrospinning,”Nano letters, vol.6, pp. 839-842,2006.

[11] J.H. He, Y. Liu, L.F. Mo, Y.Q. Wan and L.Xu, “ElectrospunNanofibres and Their Applications,”SmithersRapra Technology, 2008.